.

Observations of Quantum Erasure at a Single-Photon Level

Shiv Seshan
(Dated: May 26th 2022)

Under the Wave-Particle Duality (WPD) model, light behaves as a wave in certain circumstances and as a particle in others. To experimentally test for the presence of WPD at the level of individual photons of light, we constructed a Mach-Zehnder inteferometer, a contraption which separates a collimated source of laser light into two paths and allows the paths to subsequently interfere. By skillfully placing polarizers in the Mach-Zehnder interferometer, we could extract which-way information about the specific path a photon took through the interferometer. We found that the characteristic wave-like interference pattern of the inteferometer light was erased in the process of obtaining which-way information about individual photons of light, validating the phenomenon of quantum erasure at the single-photon level. We analyze the implications of our experiment in the two predominant interpretations of quantum mechanics: Copenhagen and Many-Worlds.

I. INTRODUCTION

A. Historical Overview

1. *Early Foundations*

Describing light is a task which has long challenged physicists. In antiquity, there was no consensus on what exactly light was; certain philosophers hypothesized light to be disturbances in a medium, while others believed it consisted of discrete, indivisible units [1]. With the advent of modern physics during the seventeenth century, the first rigorous descriptions of light arose. After founding the field of classical mechanics, Newton advanced a "corpuscular" theory in which light consisted of discrete particles [2]. Given that Newton's mechanics had already successfully accounted for the behavior of particles with mass, his particle theory of light gave scientists great hope in understanding its observed properties.

However, these hopes were dashed in the early 19th Century. In his experimental work, Young found light to exhibit properties characteristic of a wave, like interference and diffraction [3]. Across the channel, Fresnel was busy providing a theoretical edifice to Young's observations [4]. When Fresnel demonstrated that observed diffraction patterns of light could be accounted for by treating it as a transverse wave, the scientific community had all but abandoned Newton's corpuscular theory.

2. *The Photoelectric Crisis*

Amid the new physics which emerged in the nineteenth century, scientists retained their belief in the clasical wave theory of light. Nonetheless, some cracks in wave theory had become apparent by the end of the century. In 1887, Hertz observed that the kinetic energy of photoelectrons liberated from a metal lattice was independent of the intensity of the light source [5]. If light were indeed a wave, its energy would have been proportional to its intensity, so the photoelectron kinetic energy ought to have linearly increased with the *intensity* of the light. Interestingly enough, however, Hertz found the photoelectrons' kinetic energy did linearly increase as a function of a different quantity: the *intensity* of the incident light.

It took the genius of Einstein to solve this conundrum. In 1905, Einstein demonstrated that the photoelectric effect could be explained by quantizing light into discrete energy packets–photons [6]. The energy of a photon was demonstrated to be directly proportional to the frequency of light which carried it, explaining the frequency-dependence of photoelectron energy. Just over two centuries after it was published, Newton's corpuscular theory was resurrected by Einstein.

3. *The Quantum Era*

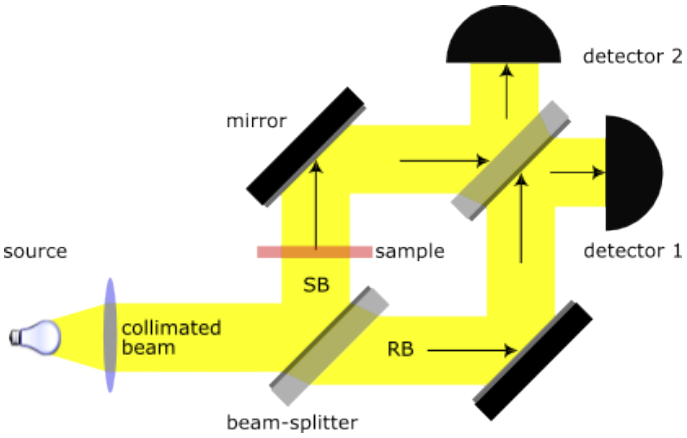

FIG. 1. A schematic of the Mach-Zehnder interferometer, depicting the two paths a particle of light can take through the interferometer.

Einstein's quantum theory of light provoked a deep philosophical crisis in physics. Light seemed to belie any attempt at characterization, for it behaved like a wave

in certain circumstances and like a particle in others, a property which came to be known as wave-particle duality (WPD).

More recent experiments in quantum mechanics have demonstrated that WPD can be induced in the simple act of measurement [7]. Consider the Mach-Zehnder interferometer, which separates a collimated source of light into two different paths, and allows those paths to subsequently interfere (Figure 1). Without any external measurements, a single photon of light which passes through a Mach-Zehnder Interferometer produces an interference pattern that is characteristic of a wave. However, if a measurement is made which–directly or indirectly–localizes the photon to a specific path in the interferometer, the photon behaves as a particle and this interference pattern is destroyed. This phenomenon, in which which-way information on the paths of photons erases interference patterns, is known as "quantum erasure."

B. Quantum Interpretations

1. *The Copenhagen Interpretation*

The Copenhagen Interpretation was among the earliest attempts to explain how the seemingly subjective process of measurement can determine how reality unfolds [8]. In contrast to the deterministic theories of physics which preceded it, the Copenhagen Interpretation views the world through a probabilistic lens. In this interpretation, any quantum state corresponds to a wave function which extends throughout a space of possible quantum states. This wave function is the generally the superposition of many "pure" states. Upon measurement of the quantum state, the wave function bizarrely "collapses" into one of its pure states. Under the Copenhagen interpretation, it is fundamentally impossible to predict how the wave function collapses before a measurement is taken. The wave function instantaneously collapses into one of its constituent pure states, with the pure states contributing most to the wave function being the most likely products of the collapse.

2. *The Many-Worlds Interpretation*

The Many-Worlds Interpretation was introduced to combat the mysticism which surrounded the collapse of the wave function in the Copenhagen Interpretation [9]. Instead of positing that physical reality unfolds like a roll of God's dice, it asserts that reality, taken as a composite whole, follows a deterministic trajectory. In each measurement of a quantum state, the Many-Worlds Interpretation states that the universe forks into multiple futures, with each future corresponding to a possible result of the measurement. In this interpretation, the randomness of quantum mechanics which any observer witnesses is an artifact of the limitations of the observer's awareness; if the observer could simultaneously witness every possible universe, he would see that all possible results of a measurement do in fact occur.

II. METHODS

A. Overview

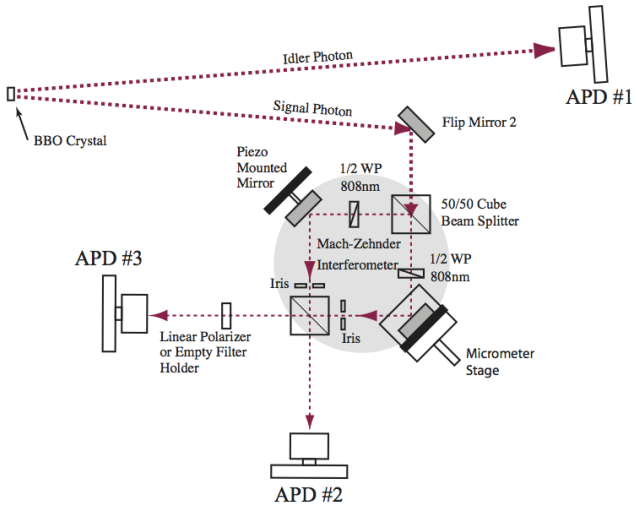

FIG. 2. A schematic of the apparatus used in the experiment [10]

We desired to observe the phenomenon of quantum erasure at a single-photon level. To this end, we built an apparatus which consisted of a vertically polarized monochromatic laser beam, a Beta Barium Borate (BBO) crystal, a Mach-Zehnder interferometer with an upper mirror mounted to a piezoelectric crystal and the lower to a micrometer, some avalanche photodetectors (APDs), and some polarizers (Figure 2).

To the nearest integer, the wavelength of the laser light is 405 nm. Through a series of mirrors, this light is directed to the BBO crystal. A small but constant fraction of the photons incident on the cyrstal excite it in such a way that it produces an entangled pair of photons as it de-excites [10]. In the de-excitation process, one of the photons, the idler photon, is aimed at the photodetector APD-1, whereas the other, the signal photon, is directed into the interferometer. In a manifestation of the conservation of energy, the wavelengths of these entangled photons are 810 ± 1 nm, double the wavelength of the exciting 405 ± 0.5 nm laser photon.

Through this setup alone, we have no which-way information on the signal photons in the interferometer; what happens to photons in the interferometer is a black box, for we take no measurements which could determine the path taken by the photon. As such, we expect to see an interference pattern characteristic of a non-localized

classical wave at APD's 2 and 3 in this setup.

To observe the presence of quantum erasure in sin photons, we needed to design our setups to:

1. indicate when a photon exhibited a wave-like int ference pattern
2. limit the probability that this interference occ from the interaction of multiple photons
3. extract which-way information about the pa taken by the photons, and confirm that the int ference pattern was erased

B. Conditions for Interference

To determine the occurrence of an interference p tern, we harnessed the namesake piezoelectric propert of the piezo crystal mounted in the interferometer. I the manufacturer, the length l of the piezo was linearly related to the applied voltage V through the following relation:

$$\Delta V = p_E \Delta l \tag{1}$$

where the piezoelectric expansion coefficient is given to be $p_E = 61 \pm 15$ nm/V

Since the piezo was oriented 45° relative to the light it received in the interferometer, from Figure 3, we can see that, for the path length difference d,

$$\Delta d = \sqrt{2}\Delta l \tag{2}$$

From Equations 1 and 2, we see

$$\frac{\sqrt{2}}{p_E}\Delta V = \Delta d \tag{3}$$

For two paths of light emerging from a collimated monochromatic source that are incident on the same detector, classical wave theory predicts the intensity I of the light is related to the path length difference d as

$$I \propto \sin(\frac{2\pi d}{\lambda}), \text{ up to a phase} \tag{4}$$

In our measurement apparatus, APD-2 and APD-3 are detectors which receive light from two different paths– the upper and lower arms of the interferometer. If only photons from the interferometer are incident on the detectors, the count rate G of the photons incident on each of these detectors is proportional to the incident intensity of light, so

$$G \propto \sin(\frac{2\pi d}{\lambda}), \text{ up to a phase} \tag{5}$$

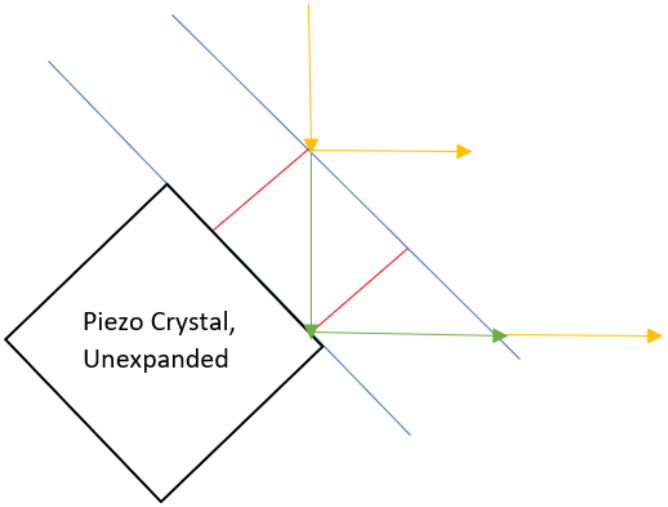

FIG. 3. The piezo is shown oriented 45° relative to the yellow arrows which represent the upper path of light in the interferometer. A change of the length of the piezo by an amount Δl in the direction of the red segments would cause the blue segment which represents the mirror to be displaced by Δl. This would alter the length of the upper path by an amount equal to the total length of the green segments, $\frac{2\Delta l}{\sin 45°} = \sqrt{2}\Delta l$. Since the length of the lower path remains constant, $\Delta d = \sqrt{2}\Delta l$.

However, due to ambient sources of light, G would provide an inflated measurement of I, since some non-signal ambient photons would be incident on APD-2 or 3. To filter out these ambient photon counts, we considered a only a subset of the photon counts on APD-2 and 3:*coincidences*. We defined a coincidence to be an event where a photon was detected at APD-2 or APD-3 within 50 ns of a detection of an photon by APD-1. Since entangled photons are simultaneously produced at the BBO crystal and traverse a size much larger than the experimental apparatus in 50 ns, a signal photon from the interferometer will almost certainly strike APD-2 or APD-3 within 50 ns of when its idler twin strikes APD-1. Moreover, it is very unlikely that an ambient photon happens to strike APD-2 or 3 within 50 ns of a detection at APD-1. Thus, the coincidence rates C_2 and C_3 of APD's 2 and 3 effectively quantify the intensity I of the light incident on these two photodetectors.

From Equation 4, we have

$$C_{2,3} \propto \sin(\frac{2\pi d}{\lambda}), \text{ up to a phase} \tag{6}$$

From the linear relationship between V and D expressed in Equation 3, we see

$$C_{2,3} \propto \sin(\frac{2\pi(\frac{\sqrt{2}}{p_E}V)}{\lambda}) \tag{7}$$

$$\propto \sin(\frac{2\pi\sqrt{2}p_E V}{\lambda}) \tag{8}$$

$$\propto \sin(\frac{2\pi V}{\frac{\lambda}{\sqrt{2}p_E}}), \text{ up to a phase} \tag{9}$$

Thus, the period T of $C_{2,3}$ as a function of V would be given by

$$T = \frac{\lambda}{\sqrt{2}p_E} \tag{10}$$

Since the uncertainties in the laser wavelength λ and the piezoelectric constant ρ_E are independent, we have the following relationship between uncertainties:

$$\delta T = \frac{\lambda}{\sqrt{2}\rho_E}\sqrt{(\frac{\delta\lambda}{\lambda})^2 + (\frac{\delta\rho_E}{\rho_E})^2} \tag{11}$$

Propagating uncertainties, we see

$$T = 9.4 \pm 2.3V \tag{12}$$

From classical wave theory, we predict that wave-like interference occurs when C_2 or C_3 exhibits a sinusoidal dependence on V, with a period of 9.4 ± 2.3 V.

C. Probability of Single-Photon Interference

A priori, there is no reason to suspect that the interference pattern we expect to see at the photodetectors are the work of a single signal photon; when two or more signal photons emitted by the BBO crystal are sufficiently physically proximate, it is possible that these signal photons can interfere with each other to produce the observed interference patterns.

To determine the likelihood that two given signal photons interfered with each other, we first estimated how densely they were spread out along a linear stretch of light in the interferometer. Since every signal photon has an idler twin, we can use the idler count rates at APD-1 to compute this density. We consistently found that idler count rates were around 90,000 counts/s. Since the efficiency of the BBO crystal in sending photons into the interferometer is almost certainly less than 1, in a stretch of light of length 3×10^8 meters, there are no more than 90,000 signal photons. Then, an upper bound of the linear density λ of signal photons along a stretch of light would be

$$\lambda = 3 * 10^{-4} \text{ photons/m} \tag{13}$$

A photon could be taken to have a radius of 50 microns, so that its "length" is 100 microns [10]. Thus, any given signal photon X would interfere with another signal photon Y provided that that Y is within a 50 micron radius of X. Then, the number of signal photons X can interfere with could be bounded by

$$\lambda_X = (3\times10^{-4} \text{ photons/m})\times(100\times10^{-6})\text{m} = 3\times10^{-8} \text{ photons} \tag{14}$$

In the de-excitation of the BBO crystal, the production of a signal photons are independent events which occur with a fixed, low probability. Thus, the number of signal photons contained within any fixed length of laser light would be distributed according to the Poisson distribution. Specifically, for the number of signal photons N contained within 50 microns of a given signal photon X, we see

$$N \sim Pois(\lambda_X) \tag{15}$$

It follows that the probability p that $N \geq 1$, i.e, the event in which there is more than one photon contained within 50 microns of X, is bounded by

$$P(N \geq 1) = 1 - P(N = 0) \tag{16}$$

$$= 1 - \frac{\lambda_X^0 e^{-\lambda_X}}{0!} \tag{17}$$

$$= 1 - e^{-\lambda_X} \tag{18}$$

$$\approx \lambda_X \text{ (from MacLaurin expansion of } e^{-x}) \tag{19}$$

$$= 3 \times 10^{-8} \tag{20}$$

Then, since p is on the order of 10^{-8} and the number of signal photons produced every second is on the order of 10^4, we would have to run the laser through the BBO crystal on the order of at least 10^4 seconds before expecting to see even one signal photon interfere with another. Since the laser was run for a much shorter duration during the experiment, we can effectively foreclose the possibility of significant levels of multi-photon interference in the experiment.

D. Extracting Which-way Information

If both half-wave plates depicted in Figure 2 are set to 0° (Setup-1), the vertically polarized laser light which enters *both* paths of the interferometer remains vertically polarized. Then, the photons which reach APD-2 and APD-3 cannot be localized, preventing us from extracting any which-way information from either detector.

However, if Setup-1 is altered so that the half-wave plate in one of the paths is set to 45° (Setup-2), the initially vertically-polarized laser light traversing the 45° path will become horizontally polarized. By placing a

vertical polarizer before APD-3, we now can localize incident photons to one of the two paths in the interferometer; if the photon transmitts through vertical polarizer and reaches APD-3, it can be traced back to the path with the 45° waveplate. Additionally, the vertically-polarized photons which reach APD-2 can be distinguished from their horizontally-polarized counterparts. Thus, in Setup 2, we can take which-way measurements at both detectors.

Finally, if the post-interferometer vertical polarizer in Setup-2 was set to be 45° (Setup 3), we would no longer be able to extract which-way information about the laser light in APD-3; the vertically polarized light of one path and horizontally polarized light of the other would be equally likely to transmit through the polarizer into APD-3 with a 45° polarization, so the photons which arrive at APD-3 provide no indication of the path they took through the interferometer. However, both vertically and horizontally polarized light continue to reach APD-2,implying that only only APD-2 performs a which-way measurement in Setup-3.

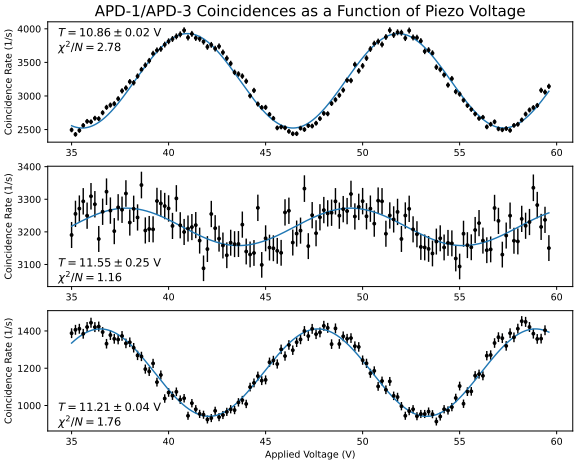

FIG. 4. Plots showing the coincidence rates C_3 between APD-1 and APD-3 in (from top to bottom) Setups 1, 2, and 3. The best-fit sinusoidal models are displayed in blue. The period parameter T of the sinusoidal model is labeled in each of the plots. The uncertainties in the data points were deduced from the coincidence rates as Poisson-distributed random variables.

Motivated by the conditions for laser light interference we deduced in Section II-B, we fit a sinusoidal model of the form

$$f(x) = A\sin(\frac{2\pi(x-c)}{T}) + b \tag{21}$$

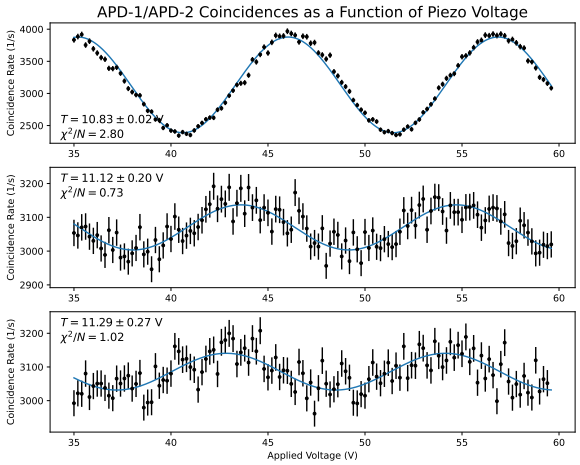

FIG. 5. Plots showing the coincidence rates C_2 between APD-1 and APD-2 in (from top to bottom) Setups 1, 2, and 3. The fits and uncertainties were determined with the same method detailed in the caption for Figure 4.

III. RESULTS

to each of the six coincidence rates plots in Figures 4 and 5. The reduced $\frac{\chi^2}{N}$ values for each of these fits were on the order of 1, suggesting that the fits effectively model the data. Additionally, the extracted periods for all of the six plots agree with the theoretically-determined value of T in (11), indicating that all six interference plots could exhibit an interference pattern.

However, there is one crucial parameter which separates the fits for C_2 in Setups-1,3 and C_3 in Setup-1 from those for C_2 in Setup-2 and C_3 in Setups-2,3: the amplitude of the sinusoid. Visibly, while the amplitudes of the fits for the former plots are clearly defined, the amplitudes of the fits for the latter plots barely exceed the uncertainties in the coincidence rate values. For this reason, we can say that interference strongly manifests for C_2 in Setups 1 and 3 and C_3 in Setup-1, but does not occur at a significant level for C_2 in Setups 2 and C_3 in Setups 2 and 3. The plots where interference does not significantly occur precisely correspond to the coincidence rates for the detectors which were identified as taking which-way measurements in in the previous section. Thus, taking which-way information destroys interference patterns, confirming the existence of quantum erasure. Moreover, from the previous section, we know it is exceedingly likely that the detected photons interfere with each other, giving us confidence in the conclusion that we observed quantum erasure at the single-photon level.

IV. DISCUSSION

The path the photon takes through the interferometer behaves like a quantum mechanical observable $\mathcal{O}$ with two eigenstates: $|+>$, which corresponds to taking the "upper" path through the interferometer, and $|->$, which corresponds to taking the "lower" path through the interferometer.

In Setup-1, no which-way measurements where performed on the photon at either APD 2 or APD 3, implying that the Setup-1 wave function Ψ_1 of the photon is a symmetric superposition of the two states

$$\Psi_1 = \frac{1}{\sqrt{2}}(|+> + |->) \tag{22}$$

In Setup-2, observers at both APD 2 and APD 3 make a which-way measurement of the photon, which causes them to see the Setup-2 wave function Ψ_2 as a pure state of either $|+>$ or $|->$. Since Ψ_2 is a localized pure state, while Ψ_1 is a delocalized mixed state, the once wave-like photon observed by APD's 2 and 3 in Setup-1 becomes partice-like in Setup-2.

The Copenhagen and Many-Worlds interpretations disagree on the process through which the mixed state Ψ_1 evolves into the pure state Ψ_2. At the moment of the which-way measurement the Copenhagen Interpretation posits that the wave function Ψ_1 spontaneously collapses into one of its pure states to become Ψ_2. Conversely, the Many-Worlds Interpretation posits that the universe itself bifurcates into two futures at the moment of the which-way measurement, where $\Psi_2 = |+>$ in one future but $|->$ in the other. Both Interpretations are entirely consistent with a sentient observer at APD 2 or 3 witnessing $\Psi_1 \rightarrow \Psi_2$, a transformation in which the wave-like interference patterns of the laser light become erased.

In Setup 3, observer at APD-3 is no longer able to take which-way measurements of detected photons, while an observer at APD-2 retains this ability. For an observer at APD-2, the particle-to-wave transformation $\Psi_1 \rightarrow \Psi_2$ accompanying the which-way measurement still occurs. However, the observer at APD-3 is incapable of making a which-way measurement since the 45° polarizer in front of the detector responds identically to vertically and horizontally polarized photons. As such, the observer at APD-3 would view the photon to be in the wave-like mixed state Ψ_1, causing a restoration of the interference pattern observed in Setup-1. Both the Copenhagen and Many-Worlds Intepretations accord a special importance to measurement, and would regard the mystical process of wave function transformation–whether understood as a collapse or as a world-bifurcation–to only occur at APD-2.

[1] D. Sedley, Lucretius, in *The Stanford Encyclopedia of Philosophy*, edited by E. N. Zalta (Metaphysics Research Lab, Stanford University, 2018) Winter 2018 ed.

[2] I. Newton, *Opticks: or, a treatise of the reflexions, refractions, inflexions and colours of light. Also two treatises of the species and magnitude of curvilinear figures* (1704).

[3] T. Young, The bakerian lecture. experiments and calculations relative to physical optics, Philosophical Transactions of the Royal Society **94**, N/A (1804).

[4] O. Darrigol, in *A History of Optics from Greek Antiquity to the Nineteenth Century*, Vol. 2, edited by O. Darrigol (Oxford University Press, Oxford, 2012) Chap. 7, pp. 220–223, 1st ed.

[5] H. Hertz, Ueber eine die electrische entladung begleitende erscheinung, Annalen der Physik **255**, 78 (1883).

[6] A. Einstein, Über einen die erzeugung und verwandlung des lichtes betreffenden heuristischen gesichtspunkt, Annalen der Physik **322**, 132 (1905).

[7] W. Reuckner and J. Peidle, Young's double slit experiment with single photons and quantum eraser, American Journal of Physics **81**, 12 (2013).

[8] J. Faye, Copenhagen Interpretation of Quantum Mechanics, in *The Stanford Encyclopedia of Philosophy*, edited by E. N. Zalta (Metaphysics Research Lab, Stanford University, 2019) Winter 2019 ed.

[9] L. Vaidman, Many-Worlds Interpretation of Quantum Mechanics, in *The Stanford Encyclopedia of Philosophy*, edited by E. N. Zalta (Metaphysics Research Lab, Stanford University, 2021) Fall 2021 ed.

[10] D. McCowan, M. Chantell, and K. van de Bogart, Uchicago instructional physics laboratories (2022).